Journal of Petroleum Science and Technology 10 (2020) 12-19
DOI:10.22078/jpst.2020.4023.1638

Journal of Petroleum Science and Technology

https://jpst.ripi.ir/

Adsorption of CH_4 and CO_2 on Cu-BDC Metal-Organic Frameworks Synthesized Using Different Solvent Separation Routes

Maryam Khalili[1], **Ensieh Ganji Babakhani**[2]*, **Armin Taheri**[3], **Mahnaz Pourkhalil**[4]

[1] *Department of Chemical Engineering, South Tehran Branch, Islamic Azad University, Tehran, Iran*
[2] *Gas Refining Technologies Division, Research Institute of Petroleum Industry (RIPI), Tehran, Iran*
[3] *Young Researcher and Elites Club, Science and Research Branch, Islamic Azad University, Tehran, Iran*
[4] *Nanotechnology Research Center, Research Institute of Petroleum Industry (RIPI), Tehran, Iran*

Abstract

Energy storage is one of the major challenges during the last decades. Natural gas adsorption on porous materials has notable advantages in comparison with the other approaches. Due to the lack of adsorption information about Cu-BDC (copper terephthalate), it was synthesized by two different solvent separation procedures and identified using X-ray diffraction (XRD), Brunauer-Emmet-Telller (BET) and thermogravimetric analysis (TGA) techniques. Moreover, equilibrium adsorption measurements were performed for CH_4 and CO_2 gases in the pressure range 0-50 bar at two various temperatures (293 and 323 K), and experimental adsorption data were modeled with adsorption isotherms. Also, the sample synthesized by the new solvent separation procedure had 918 m^2/gr surface area and 0.42 cm3/gr pore volume which were respectively 45% and 50% higher than the traditional method. In addition, this sample has shown CO_2 and CH_4 adsorption capacity (16.72 and 13.23 mmol gr^{-1}) were desirable in comparison with other conventional Metal-Organic Frameworks (MOFs) and its methane adsorption value was close to DOE (Department of Energy) targets. To investigate the application of the synthesized materials, the selectivity of CO_2/CH_4 was determined by IAST (ideal adsorbed solution theory) according to the sorption test information of the single components. Finally, adsorption enthalpy of the adsorbates on the two samples was computed using the Clausius-Clapeyron equation and the results were in accordance with the isotherms at two various temperatures (293 and 323 K).

Key words: Metal-Organic Frameworks (MOF), Adsorbed Natural Gas (ANG), Methane, Carbon dioxide, Adsorption.

Introduction

Energy storage is one of the major challenges that have been faced by chemists during the last decades. Natural gas (NG) has a notable advantage in comparison with ordinary fossil fuels from the environmental and large quantity of resource points of view. Natural gas is mostly made up of methane, with a high ignition heat, and it releases the smallest amount of carbon dioxide among the other fossil sources. Additionally, methane has the most H/C ratio, so it has a higher octane number than other fuels. Therefore, one of the important issues is further improvement of natural gas storage [1-3].

In recent years, three important NG storage forms have been suggested: (a) liquefied natural gas (LNG), (b) compressed natural gas (CNG), and (c) adsorbed natural gas (ANG) [1,4]. Due to the very low liquefaction temperature of methane, LNG is obtained by cryogenic expensive techniques and high-cost refueling facilities have inhibited its comprehensive commercial applications [1,3,4]. CNG is a supercritical fluid at room temperature under 200–300 bar pressure in steel vessels. In addition to this fact that CNG volumetric energy is about 2.6 times lower than LNG, the high cost of the high-pressure conditions and leakage of refueling stations are generally great drawbacks that need to be considered [4,5].

Therefore, the other approaches of methane storage have been investigated in the last decade. ANG is methane storage on porous materials under room temperature and the pressure of 35 bar. The chance of gas distribution from urban or local pipelines, using reasonable equipment with better safety than LNG and CNG, are some of special interests of ANG technology [3,4].

To elevate the usage of CH4, the U.S. Department of Energy (DOE) has fixed the purpose for methane storage at 180 v(STP)/v (standard temperature and pressure equal to the volume of methane per volume of the adsorbent) under 35 bar pressure and near ambient temperature. In this condition, the energy density of ANG is equal to CNG [1,9,10].

**Corresponding author:* Ensieh Ganji Babakhani, Gas Refining Technologies Division, Research Institute of Petroleum Industry, Tehran *(RIPI)*, Iran
E-mail addresses: ganjie@ripi.ir

Received 2020-02-03, Received in revised form 2020-07, Accepted 2020-08-17, Available online 2020-11-22

On the other hand, because of increasing CO_2 amounts in the atmosphere, global temperature is expected to rise about 2-4 ºC by 2050 [6]. One of the ways of reducing CO_2 emissions is using carbon capture and storage (CCS) technologies. At the moment, CCS technologies are not sufficiently convincing because of their high cost. Therefore, many studies are conducted to modify present methods or make new ones. Chemical absorption by amine is a common method in the industry, but it has caused some problems such as absorbents regeneration high energy demand, and decrease in capability over time because of their low thermal stability. Furthermore, solvent-based methods are not environmentally friendly all the time. These issues result in a continuous search to find better ways of CO_2 capture. Physical adsorption on porous materials has been reported as a good method for high CO_2 adsorption capacity at ambient temperature [6-8].

Currently, the storage of CH_4 and CO_2 gases in porous solids has been studied as a promising method. Accordingly, suitable new materials for gas adsorption purposes are an interesting field of investigation. High specific surface area is one of the most important properties that a suitable material for gas storage should have (Like porous solids). However, the other properties should be considered as well [1].

Several types of porous solids such as carbon nanotubes, porous polymers, porous ceramics, zeolites, and activated carbon have been studied already as potential storage media for mentioned gases [1,11- 13]. Furthermore, zeolites represent methane adsorption below 100 cm3 (STP)•cm^{-3}, while most porous carbon materials exhibit the range of 50–160 cm^3(STP)•cm^{-3} [14]. These results are far from the DOE purpose for methane storage. Therefore, study on further porous materials is still an attractive field of activity.

A new category of crystalline porous materials named Metal-Organic Frameworks (MOFs) is made from a three-dimensional structure (metal-oxide clusters connected to organic ligands), which is suitable for gas storage purpose. Some of their advantages such as the possibility of structure engineering (by suitable choice of ligand and metal), high surface area and pore volume, and the promising gas adsorption values have attracted the academic and industrial attention. Reasonable costs, high purity, and crystalline structure of these materials cause a remarkable interest in using them in ANG technology [4,6].

The nickel terephthalate, which has been synthesized in 1967 by Acheson and Galwey, is the first compound from metal salt and terephthalic acid (tpaH) [15]. Also, other metal terephthalates compounds were synthesized by Sherif [16]. One of the synthesized compositions in primary years was Cu(tpa)•3(H_2O). Its conductivity and magnetic susceptibility were studied by Cueto et al [17,18]. But the first studies about copper terephthalate surface area were publicized by Mori et al [19].

Recently, researchers have provided MOFs with higher porosities using copper terephthalate and triethylenediamine or dimethylamine. Attractive features of Cu(tpa) MOF make it a preferred substance for gas adsorption purposes [18,20]. However, information about gas adsorption isotherms of copper terephthalate has been published rarely, and there is a limited investigation on it. Although, the structures of copper terephthalates were studied, no different methods of synthesis have been reported.

Previously, many MOFs have been synthesized by hydrothermal methods. These approaches have some drawbacks: MOF structure collapsing and surface area reduction because of metal terephthalates dehydration [18]. The interesting features of N, N-dimethylformamide (DMF) such as high boiling point and good capability to dissolve metal salts and carboxylic acid made it a desirable solvent. Improving solvent separation methods could be an interesting subject of studies. Soxhlet extractor method (a rarely used method) was suggested by Chowdhury et al. for better extraction of DMF solvent and consequently higher pore volume and surface area [21].

Herein, the synthesis and characterization of two Cu-BDC samples under solvothermal conditions have been presented by us in which their solvent separation methods are different. Then the adsorption assessment of nitrogen, methane, and carbon dioxide on the synthesized samples has been studied. A set of structural assessment analysis, experimental adsorption outcomes, and adsorption isotherms modeling were applied to exhibit the synthesis and solvent separation method effect on the properties and gas adsorption capacity of CO_2 and CH_4, which they are still missing in literature until today. This study leads to the modification of MOFs with favorable adsorption properties.

Materials and Methods

Materials

Copper (II) nitrate trihydrate [$Cu\ (NO_3)_2\ .3H_2O$ (99%, Merck)], Benzene-1,4-dicarboxylic acid (commonly known as Terephthalic acid) [98%, Merck], N, N-dimethylformamide [99.8%, Merck], and methanol [99.5%, Merck] were used as got from the seller.

Synthesis Procedure

A mixture of $Cu(NO_3)_2\ .3H_2O$ (1.75 g, 4.35 mmol), Benzene-1,4-dicarboxylic acid (1.203 g, 4.35 mmol), and DMF (150 mL) was stirred at room temperature for about 10 minutes. This mixture was heated to 110 °C for 36 h into a teflon-lined steel autoclave. Then the autoclave was cooled naturally to room temperature. In the common method, Cu-BDC blue crystals were recovered by centrifuging and washing with DMF followed by drying at 30 °C under vacuum overnight (sample A). Whereas in the new method, blue precipitated crystals were separated by the common method. Afterwards, using a Soxhlet extractor, the DMF was removed with methanol overnight. After that, the product was dried under vacuum condition and at room temperature for 12 h (sample B).

Characterization

The MOFs structures were recognized by X-ray diffraction (XRD) on a Philips pw1729 diffractometer. To study the thermal stability of the products, thermogravimetric analysis (TGA) was taken on the samples using a TGA/ SDTA 851e at a heating rate of 5 $°C\cdot min^{-1}$ under N_2. The N_2 physisorption analysis at 77 K was performed for measuring surface area and the pore volume in Micromeritics Tri Star II 3020. The samples were out-gassed under vacuum at 453 K for about 3h. Also, relative pressure (P/P0) range of 0.05–0.2 was used in the BET surface area calculation, and $P/P0 > 0.98$ was considered for pore volume calculation.

Adsorption Equilibrium Measurements

CH_4 and CO_2 equilibrium adsorption of the two Cu-BDC samples were measured volumetrically at 293 and 323 K. He, CH_4 and CO_2 were used in this study which their purities were 99.99%, 99.95%, and 99.90% respectively. Gas adsorption isotherm measurement was done by the volumetric method at pressures up to 50 bars and using the setup shown in Fig. 1. In common methods, the weight of the sample is used for the adsorption calculations. The specified amount of adsorbent was filled in the adsorption cell and attached to the setup. Prior to the measurement, the sample was degassed at 180 °C for 3 h under vacuum.

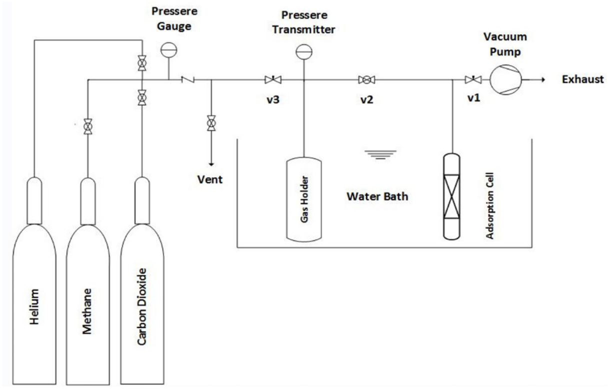

Fig. 1 Adsorption test setup.

For adsorption assessment, the temperature was kept constant by using a water bath at 293 and 323 K during the measurement. At first, the holding cell was filled by the adsorbate gas to a certain pressure. The sorption tests were performed with changing the pressure of the holder cell. The pressure changes with time were recorded in a PC using a data acquisition system. The pressure of the adsorption cell decreased due to gas adsorption. Helium gas was used to measure dead volume while it is assumed that helium is not adsorbed on the adsorbent. The exact pressure reduction that belongs to the gas adsorption could be calculated by evaluating the dead volumes and measuring pressure changes [22-24].

Results and Discussion

Material characterization

Powder X-ray diffraction analysis of the porous materials was performed to ensure high purity of the crystalline phases. XRD patterns are shown in Fig. 2. A good crystallinity was shown for both samples. The published literature data confirmed the main peaks appeared at 10°-30° (2Θ), and the diffraction peaks do not show the existence of such impurity [18].

Thermogravimetric analysis (TGA) of MOF samples is shown in Fig. 3. The thermogravimetric diagram of Sample A shows a clear weight-loss step that has started at 150 °C and has ended at 200 °C, which it belongs to the loss of DMF molecules as the solvent. The consistency of the adsorbent higher than 220 °C is shown by no remarkable weight changes until the pyrolysis at 325 °C [18]. The first weight loss of Sample B occurs between 250 and 300 °C. The absence of any other weight change until 220 °C indicating that DMF molecules is completely removed by the Soxhlet extractor with methanol from pores and surface of the sample. Furthermore, the weight loss step higher than 380 °C, corresponds to the BDC removal from the framework, collapse of the crystal structure, and consequently decomposition of the sample. The results of the BET surface area and pore volume amounts obtained from the nitrogen physisorption isotherms at 77 K are demonstrated in Fig. 4 and Table 1. According to the IUPAC classification, both samples express microporosity as the reversible type I(a) adsorption isotherms corresponding to the microporous materials [25].

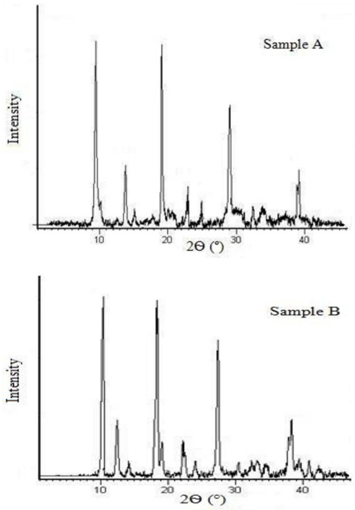

Fig. 2 Samples X-ray diffraction patterns.

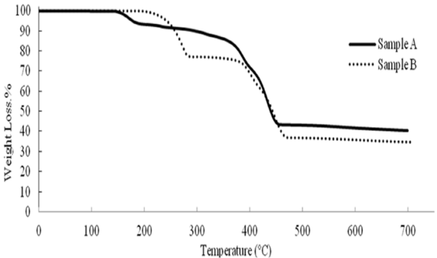

Fig. 3 TGA analysis with the heating rate of 5 °C·min^{-1} under the air atmosphere.

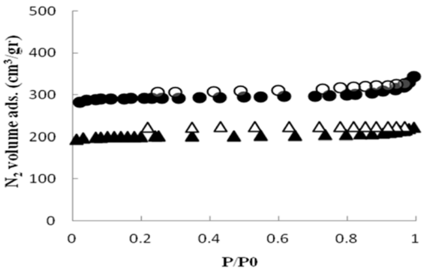

Fig. 4 Nitrogen adsorption and desorption at 77 K. (Δ): Sample A and (o): Sample B.

Table 1 Samples surface area and pore volume.

Sample	BET surface area (m^2/gr)	Pore volume (cm^3/gr)
Sample A (in this study)	603	0.29
Sample B (in this study)	918	0.42
Carson et al [18]	625	0.28

The quick saturation step at relatively low pressure (<0.02 P/P0) signifies micropore filling. In addition, isotherms without hysteresis loop illustrate a high microporosity structure and stability of the samples [26]. The maximum nitrogen uptake capacities at P/P0 = 0.99 for samples A and B were 212 and 326 cm3 g^{-1} respectively. These amounts had good similarity to the reported surface areas by Carson and Kenji for Cu(tpa) [18, 27].

The high porosity is one of the most essential features of MOFs, which involves the number of adsorptive sites within a given porous material. The work clarifies the aspect of the synthesis procedure in the pore volume of MOFs exhibiting the exceptional porosity. According to our experimental results (Table 1), it was found out that sample B possesses the largest pore volume.

Gas Adsorption

CH_4 and CO_2 gases adsorption isotherms on both samples at two various temperatures are given in Fig. 5. According to the IUPAC classification, all samples exhibit type I(a) adsorption isotherms that corresponds to the microporous materials [25]. As it was expected, due to the exothermic nature of adsorption the increase in temperature reduces the adsorption capacity. The adsorption capacity for CH_4 at 35 bars and 293 K on samples A and B amounts to 11.58 and 13.23 mmol gr^{-1} respectively. Moreover, CH_4 adsorption capability has a strong relation with surface area and pore volume in porous solids (such as MOFs) [28]. Therefore, the CH_4 adsorption amount of sample B is higher than sample A.

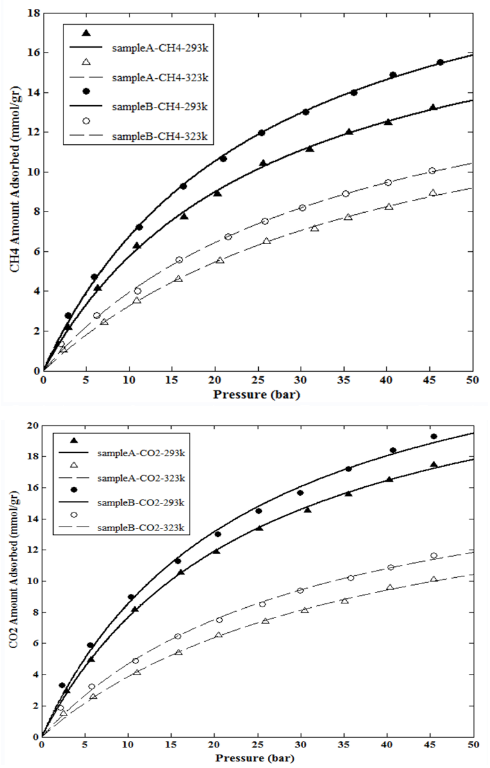

Fig. 5 Adsorption isotherms for CH_4 and CO_2 on the synthesized samples; Symbols: Experimental data; Lines: Langmuir model fitting.

As seen in Fig. 5, carbon dioxide uptake on samples A and B were 14.61 and 16.72 mmol g-1 respectively. Therefore, it is concluded that the CO_2 adsorption amount is higher than that of CH_4 under the same conditions as it was observed for both samples. This observation can be attributed to the adsorption mechanism which is related to the physical properties of gas molecules, such as quadrupole moment or polarizability [29]. Higher CO_2 adsorption is expected due to its higher polarizability and quadrupole moment in comparison to CH_4. In other words, higher CO_2 adsorption quantities exhibit strong interactions (affinity) between both samples and this molecule. Non-polar nature of CH_4 molecules in comparison to the polar nature of CO_2 is the reason for these results. The larger electrostatic interaction between CO_2 and MOF surface caused to higher uptake [24,30,31]. Also, the adsorption capacities of sample B for both gases were higher than sample A. This is related to the higher BET surface area and pore volume of sample B obtained using the Soxhlet extractor method.

CH_4 and CO_2 adsorption of samples A and B were compared with those of other MOFs synthesized with BDC ligand in Table 2. CO_2 and CH_4 uptakes of the synthesized samples in this study at 293 K and 35 bars was at a good level in comparison with the well-known MOFs. Methane adsorption of sample B was extremely higher than the other MOFs, so it could meet the requirements of DOE (Department OF Energy) as a suitable choice for ANG applications.

Modeling

CH_4 and CO_2 adsorption isotherms on both samples were fitted with three well-known isotherms models, Langmuir (Equation 1), Freundlich (Equation 2) and Temkin (Equation 3) using Matlab software (MATLAB 9.0.0 (R2016a)). Obtained adjustable parameters for pure methane and carbon dioxide at 293 and 343 K are mentioned in Tables 3 and 4.

$$q_e = \frac{q_m bp}{1+bp} \tag{1}$$

$$q_e = k_f p^{\frac{1}{n}} \tag{2}$$

$$q_e = \beta In(AP) \tag{3}$$

where q_e is adsorbed amount per mass of adsorbent (mmol/g), q_m is maximum adsorbent capacity (mmol/g), P is equilibrate gas pressure with adsorbed phase (bar), b is affinity coefficient (bar^{-1}), Kf is freundlich isotherm constant (mmol/g), n is adsorption intensity, β is a constant related to adsorption heat (mmol/g), and A is Temkin isotherm equilibrium binding constant (bar^{-1}).

Based on the estimated R-squared values for the Langmuir model, experimental adsorption data and model results are in good accordance with each other. In Fig. 5, the fit lines obtained using the Langmuir model and experimental data have been shown. As methane is a non-polar gas, and it tends to adsorbed on homogeneous surfaces and according to the reported assumptions of this model and R-squared values, the homogeneity of the synthesized adsorbents is confirmed. Maximum adsorption capacity (q_m) of pure gases, which was calculated from the Langmuir model, was considerably better than that reported earlier in literature, and it indicates that if the pressure increases, how much gas will be adsorbed [1,21,35-37].

In line with the amount of affinity coefficient (*b*) in the Langmuir model, the value of parameter b represents a fair slope at the beginning of the absorption isotherm curve, which it represents a high interaction between the adsorbate and the absorbent. Regarding the use of adsorbents for adsorption and desorption cycles, the lower Langmuir parameter b means that the absorbent recovery would be performed easier and much energy would not be required for desorption operations.

Table 2 Comparison of CH_4 and CO_2 adsorption for different porous materials.

Samples	CH_4 adsorption capacity (mmol/gr)	CO_2 adsorption capacity (mmol/gr)	Temperature(K)	Pressure(bar)	Reference
MIL-53-Al	6.65	10	304	25	[32]
MIL-53-Cr	7.10	10	304	25	[32]
IRMOF-6	10.68	19.8	298	40	[33]
IRMOF-1	10	21.7	298	35	[33]
MIL-100	7.56	18	304	50	[34]
MIL-101	10.12	40	304	50	[35]
MOF-5	7.5	---	298	36	[22]
PCN-14	11.81	---	290	35	[9]
MIL-53-Cu	8.52	---	298	35	[30]
Sample A	11.58	14.61	293	35	This study
Sample B	13.23	16.72	293	35	This study

Table 3 Langmuir, Freundlich, and Temkin adsorption parameters of CH_4 and CO_2 on the synthesized samples at 293 K.

Parameter	Sample	CH_4			CO_2		
		Langmuir	Freundlich	Temkin	Langmuir	Freundlich	Temkin
q_m	A	20.62	-	-	26.56	-	-
	B	23.95	-	-	28.69	-	-
b	A	0.0384	-	-	0.0407	-	-
	B	0.0394	-	-	0.0426	-	-
k_f	A	-	1.561	-	-	2.106	-
	B	-	1.875	-	-	2.44	-
n	A	-	1.759	-	-	1.78	-
	B	-	1.784	-	-	1.829	-
β	A	-	-	4.16	-	-	5.399
	B	-	-	4.695	-	-	5.535
A	A	-	-	0.4689	-	-	0.4877
	B	-	-	0.463	-	-	0.5851
R^2	A	0.9983	0.9896	0.9810	0.9991	0.9899	0.9817
	B	0.9987	0.9921	0.9733	0.9950	0.9965	0.9694

Table 4 Langmuir, Freundlich, and Temkin adsorption parameters of CH_4 and CO_2 on the synthesized samples at 323 K.

Parameter	Sample	CH_4			CO_2		
		Langmuir	Freundlich	Temkin	Langmuir	Freundlich	Temkin
q_m	A	16.85	-	-	18.12	-	-
	B	17.74	-	-	19.24	-	-
b	A	0.0240	-	-	0.0271	-	-
	B	0.0286	-	-	0.0322	-	-
k_f	A	-	0.7377	-	-	0.9215	-
	B	-	0.9676	-	-	1.220	-
n	A	-	1.522	-	-	1.579	-
	B	-	1.610	-	-	1.682	-
β	A	-	-	2.721	-	-	3.100
	B	-	-	2.944	-	-	3.327
A	A	-	-	0.4377	-	-	0.4504
	B	-	-	0.5203	-	-	0.548
R^2	A	0.9987	0.9963	0.9425	0.9976	0.9963	0.9519
	B	0.9969	0.9948	0.9396	0.9944	0.9978	0.9453

In general, for an ideal absorbent, the high q_m and fair slope of isotherm adsorption are desirable. With respect to the BET results, both samples had excellent reversibility of N_2, and the initial adsorption capacity has been preserved. In addition, the quantities of q_m and b parameters of CH_4 and CO_2 uptake show the desired adsorption.

Freundlich and Temkin adsorption isotherms are generally used to define adsorption specification of heterogeneous surfaces. In the Freundlich model, the constant K_f is an index of the adsorption capability, while 1/n is a function of the adsorption intensity. If n=1 then the tendency between surface and adsorbent is not related to the concentration. If the value of 1/n is lower than 1, it indicates normal adsorption. However, 1/n being more than one represents collective adsorption. But Freundlich adsorption isotherm fails at high pressure because by increasing the pressure, it has a maximum without limitation. When temperature increases, the adsorbed amount rises more slowly, and higher pressures are needed to saturate the surface. If 1<n<10, the sorption process will be desirable, while 1/n is a heterogeneity parameter. The smaller 1/n represents more heterogeneity [38,39]. In this study, the parameter n is between one and two, which it indicates that the adsorption is favorable, and the surface has not shown heterogenisity. The R-squared value of Freundlich isotherm and specially Temkin isotherm is less fitted with experimental data in comparison with Langmuir isotherm. It represents that the surface of samples A and B is homogeneous.

As a further assessment, the selectivity of the equimolar CO_2/CH_4 mixture was estimated using the Langmuir equation and the IAST (Ideal Adsorbed Solution Theory) which proposed by Myers and Praunitz [40]. It is applied for prediction of the adsorption selectivity and the multi-component isotherm of gas mixtures. The equilibrium selectivity factor (S_{ij}) is defined as:

$$S_{ij} = \frac{x_i / x_j}{y_i / y_j} \tag{4}$$

where:

x_i and x_j are the mole fractions of the two components on the adsorbent, and

y_i and y_j are the corresponding mole fractions in the gas phase.

Which the calculations of an equimolar gas mixture were as below:

$$x_i = \frac{n_i}{n_{total}} \tag{5}$$

$$x_j = 1 - x_i \tag{6}$$

$$n_{i,j} = \frac{(q_{m_{i,j}} * b_{i,j} * y_{i,j} * p)}{1 + (b_i * y_i * P + b_j * y_j * p)} \tag{7}$$

$$n_t = n_i + n_j \tag{8}$$

To evaluate the ideal selectivity of the samples under binary gas mixture (i: CO_2; j: CH_4), the IAST model with the obtained fitted parameters of Langmuir isotherm (Tables 3 and 4) was applied, and the equations were solved by MATLAB software.

The obtained selectivity of the mixture versus pressure is shown in Fig. 6. Moreover, CO_2 selectivity increases by rising total pressure from 1 to 40 bars. The selectivity is always larger than 1 in the entire pressure which proves that both samples are selective for CO_2 versus CH_4. As explained above, this is related to the higher affinity (b) and saturation capacity (q_m) of CO_2 than those of CH_4. The selectivity of two samples (A and B) is near to each other. The little decrease in the selectivity of sample B with respect to A at 293 K and the similar selectivity of two samples at 323 K could be related to the increase in non-selective sites of adsorbent (resulted in non-selective adsorption mechanism) while they are holding the same number of selective sites.

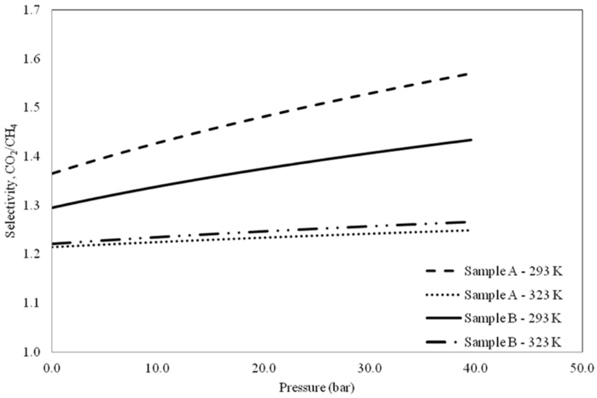

Fig. 6 The predicted IAST selectivity of CO_2/CH_4 as a function of pressure for samples A and B.

Adsorption enthalpy of adsorbates on the samples was calculated using the Clausius-Clapeyron equation according to the pure gas isotherms at 293 and 323 K, as seen in Fig. 7. The heat of adsorption (enthalpy) identifies the interaction between the gas molecules and the adsorbent surface. Adsorption enthalpies for both gases on the samples slightly increase by loading because of an increase in binding energy between gas molecules and adsorbent at the high-pressure region. Higher enthalpy values of CO_2 can be attributed to the polar nature of CO_2 molecules in comparison with the non-polar nature of CH_4. Furthermore, adsorption enthalpy of sample A for CO_2 and CH_4 at zero loading was about 23.2 kJ/mol and 13.3 kJ/mol respectively. Whereas they were 17.4 kJ/mol and 10.1 kJ/mol for sample B. The enthalpies on sample B were smaller than A, and these results is in accordance with the selectivity data. Regeneration of MOFs would be easier with lower values of adsorption enthalpies. However, it is noted that the low adsorption heat at zero coverage indicates a weak gas-MOF interaction, and thus gas uptake would be small in low-pressure conditions.

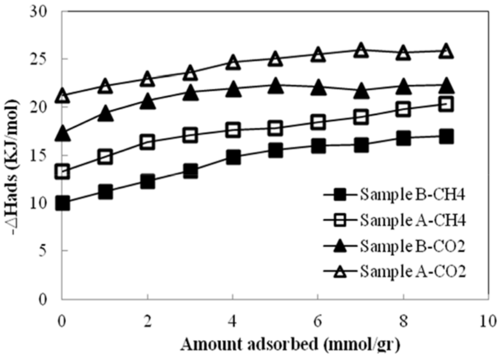

Fig. 7 Variation of adsorption enthalpy with loading on samples for CO_2 and CH_4. Lines are drawn as a guide to the eye.

Conclusions

In this study, Cu-BDC metal-organic frameworks were synthesized using a solvothermal method via two different solvent separation procedures. The products were identified by XRD, BET, and TGA techniques. Sample B pore volume and surface area were extremely higher than sample A because of using Soxhlet extractor to remove DMF from the adsorbent pores. Moreover, CH_4 and CO_2 adsorption were taken on the samples in the pressure range of 0 to 50 bars and two various temperatures. Experimental data were fitted well with Langmuir isotherm, and homogeneity of the synthesized adsorbents was confirmed. The adsorption capacity of both samples was comparable to the other conventional MOFs, and methane adsorption value of sample B was near to the DOE technical targets, so it is suggested as a promising MOF for using in ANG applications. CO_2/CH_4 selectivity was determined by IAST (ideal adsorbed solution theory). Ultimately, the results illustrated that the samples were selective for CO_2 over CH_4. In addition, adsorption enthalpy of adsorbates presented a good tendency of gas uptake, and they would be regenerated easily according to reversibility result of BET and adsorption enthalpies values.

Nomenclatures

ANG: Adsorbed natural gas
BET: Brunauer-emmet-telller
CCS: Carbon capture and storage
DOE: Department of energy
IAST: Ideal adsorbed solution theory
LNG: Liquefied natural gas
MOF: Metal-organic frameworks
TGA: Thermogravimetric analysis
XRD: X-ray diffraction

References

1. Senkovska I, Kaskel S (2008) High pressure methane adsorption in the metal-organic frameworks $Cu_3(btc)_2$, $Zn_2(bdc)_2$dabco, and $Cr_3F(H_2O)_2O(bdc)_3$, Microporous and Mesoporous Materials, 112, 1–3: 108-115.
2. Alcañiz-Monge J, De La Casa-Lillo MA, Cazorla-Amorós D, Linares-Solano A (1997) Methane storage in activated carbon fibres, Carbon, 35, 2: 291-297.
3. Lozano-Castelló D, Alcaniz-Monge J, De la Casa-Lillo MA, Cazorla-Amoros D, Linares-Solano A (2002) Advances in the study of methane storage in porous carbonaceous materials, Journal of Fuel, 81, 14: 1777-1803.
4. Tagliabue M, Rizzo C, Millini R, Blom R, Zanardi S (2011) Methane storage on CPO-27-Ni pellets, Journal of Porous Materials, 18, 3: 289-296.
5. Cracknell RF, Gordon P, Gubbins KE (1993) Influence of pore geometry on the design of microporous materials for methane storage, The Journal of Physical Chemistry, 97, 2: 494-499.
6. Liang Z, Marshall M, Chaffee AL (2009) Comparison of Cu-BTC and zeolite 13X for adsorbent based CO_2 separation, Energy Procedia, 1, 1: 1265-1271.
7. Lee J.Y, Wood C, Bradshaw D, Rosseinsky M, Cooper A (2006) Hydrogen adsorption in microporous hypercrosslinked polymers, Chemical Communications, 25: 2670-2672.
8. Dietzel PDC, Besikiotis V, Blom R (2009) Application of metal-organic frameworks with coordinatively unsaturated metal sites in storage and separation of methane and carbon dioxide, Journal of Materials Chemistry, 19, 39: 7362-7370.
9. Ma S, Sun D, Simmons J, Collier C, Yuan D, Zhou H (2008) Metal-organic framework from an anthracene derivative containing nanoscopic cages exhibiting high methane uptake, Journal of the American Chemical Society, 130, 3: 1012-1016.
10. Burchell T, Rogers M (2000) Low pressure storage of natural gas for vehicular applications, Energy Efficiency and Renewable Energy, SAE International, 109, 4: 2242-2246.
11. Muris M, Pavlovsky N, Bienfait M, Zeppenfeld P (2001) Where are the molecules adsorbed on single-walled nanotubes?, Surface Science, 492, 1–2: 67-74.
12. Dunne JA, Rao M, Sircar S, Gorte RJ, Myers AL (1996) Calorimetric heats of adsorption and adsorption isotherms. 2. O_2, N_2, Ar, CO_2, CH_4, C_2H_6, and SF_6 on NaX, H-ZSM-5, and Na-ZSM-5 Zeolites, Langmuir, 12, 24: 5896-5904.
13. MacDonald JAF and Quinn DF (1995) The preparation of active carbons from natural materials for use in gas storage, Journal of Porous Materials, 1, 1: 43-54.
14. Pfeifer P, Burress JW, Wood MB, Lapilli CM, Barker SA, Pobst JS, Cepel RJ, Wexler C, Shah PS, Gordon MJ, Suppes GJ (2008) High-surface-area biocarbons for reversible on-board storage of natural gas and hydrogen, Materials Research Society symposia proceedings, 1041, 2: 63.
15. Acheson RJ, Galwey AK (1967) The thermal decomposition of nickel terephthalate and nickel salts of other carboxylic acids, Journal of the Chemical Society A: Inorganic, Physical, Theoretical, 0: 1174-1178.
16. Sherif FG (1970) Heavy Metal Terephthalates, Industrial and Engineering Chemistry Product Research and Development, 9, 3: 408-412.
17. Cueto S, Gramlich V, Petter W, Rys FS, Rys P (1991) Structure of copper(II) terephthalate trihydrate, Acta Crystallographica Section C, 47, 1: 75-78.
18. Carson CG, Hardcastle K, Schwartz J, Liu X, Hoffmann C, Gerhardt RA, Tannenbaum R (2009) Synthesis and structure characterization of copper terephthalate metal–organic frameworks, European Journal of Inorganic Chemistry, 16: 2338-2343.
19. Wasuke M, Fumie I, Keiko Y, Hirokazu N, Satoshi T, Michihiko K (1997) Synthesis of new adsorbent copper(II) terephthalate, Chemistry Letters, 26, 12: 1219-1220.
20. Seki K (2001) Design of an adsorbent with an ideal pore structure for methane adsorption using metal complexes, Chemical Communications, 30, 16: 1496-1497.
21. Chowdhury P, Bikkina C, Meister D, Dreisbach F (2009) Comparison of adsorption isotherms on Cu-BTC metal organic frameworks synthesized from different routes, Microporous and Mesoporous Materials, 117, 1–2: 406-413.
22. Mohamed Eddaoudi JK, Nathaniel Rosi, David Vodak,

Joseph Wachter, Michael O'Keeffe, and Omar M. Yaghi (2002) Systematic design of pore size and functionality in isoreticular MOFs and their application in methane storage, Science, 295: 469

23. Taheri A, Babakhani E, Towfighi J (2018) Study of synthesis parameters of MIL-53(Al) using experimental design methodology for CO_2/CH_4 separation. Adsorption Science & Technology, 36, 1-2: 247-269.
24. Taheri A, Babakhani E, Towfighi J (2017) A MIL-101(Cr) and graphene oxide composite for methane-rich stream treatment, Energy and Fuels, 31, 8: 8792-8802.
25. Thommes M, Kaneko K, Neimark A, Olivier J, Rodriguez F, Rouquerol J, Sing K (2015) Physisorption of gases, with special reference to the evaluation of surface area and pore size distribution (IUPAC Technical Report), Pure and Applied Chemistry, 87, 9-10.
26. Basu S, Cano-Odena A, Vankelecom IFJ (2010) Asymmetric matrimid®/[$Cu_3(BTC)_2$] mixed-matrix membranes for gas separations, Journal of Membrane Science, 362, 1: 478-487.
27. Kenji S, Satoshi T, Wasuke M (2001) Characterization of microporous copper(II) dicarboxylates (Fumarate, terephthalate, and trans-1,4-cyclohexanedicarboxylate) by gas adsorption, Chemistry Letters, 30, 2: 122-123.
28. Llewellyn PL, Maurin G (2005) Gas adsorption microcalorimetry and modelling to characterise zeolites and related materials, Comptes Rendus Chimie, 8, 3: 283-302.
29. Chaemchuen S, Zhou K, Yao C, Ke X, Tendeloo GV, Verpoort F (2015) Tuning metal sites of DABCO MOF for gas purification at ambient conditions, Microporous and Mesoporous Materials, 201, 0: 277-285.
30. Anbia M, Sheykhi S (2012) Synthesis of nanoporous copper terephthalate [MIL-53(Cu)] as a novel methane-storage adsorbent, Journal of Natural Gas Chemistry, 21, 6: 680-684.
31. Li J-R, Ma Y, McCarthy M, Sculley J, Yu J, Jeong H, Zhou H (2011) Carbon dioxide capture-related gas adsorption and separation in metal-organic frameworks, Coordination Chemistry Reviews, 255, 15: 1791-1823.
32. Bourrelly S, Llewellyn P, Serre C, Millange F (2005) Different adsorption behaviors of methane and carbon dioxide in the isotypic nanoporous metal terephthalates MIL-53 and MIL-47, Journal of the American Chemical Society, 127, 39: 13519-13521.
33. Millward AR and Yaghi OM (2005), Metal-organic frameworks with exceptionally high capacity for storage of carbon dioxide at room temperature, Journal of the American Chemical Society, 127, 51: 17998-9.
34. Llewellyn PL, Bourrelly S, Serre C, Vimont A (2008) High uptakes of CO_2 and CH_4 in Mesoporous Metal-Organic Frameworks MIL-100 and MIL-101, Langmuir, 24, 14: 7245-7250.
35. Chowdhury P, Mekala S, Dreisbach F, Gumma S (2012) Adsorption of CO, CO_2 and CH_4 on Cu-BTC and MIL-101 metal organic frameworks: Effect of open metal sites and adsorbate polarity, Microporous and Mesoporous Materials, 152, 0: 246-252.
36. Mishra P, Edubilli S, Mandal B, Gumma S (2013) Adsorption of CO_2, CO, CH_4 and N_2 on DABCO based metal organic frameworks, Microporous and Mesoporous Materials, 169, 0: 75-80.
37. Wang H, Getzschmann H, Senkovska I, Kaskel S (2008) Structural transformation and high pressure methane adsorption of Co2(1,4-bdc)2dabco, Microporous and Mesoporous Materials, 116, 1–3: 653-657.
38. Bolis V (2013) Fundamentals in adsorption at the solid-gas interface, Concepts and Thermodynamics, in Calorimetry and Thermal Methods in Catalysis, Springer Berlin Heidelberg: Berlin, Heidelberg, 3-50.
39. Dada AO, Olalekan AP, Olatunya AM, DADA O (2012) Langmuir, freundlich, temkin and dubinin–radushkevich isotherms studies of equilibrium sorption of Zn2+ unto phosphoric acid modified rice husk, IOSR Journal of Applied Chemistry, 3, 1: 38-45.
40. Duong DD (1998) Adsorption analysis: equilibria and kinetics (1st edition), Imperial College Press, 2: 201-202.